LAWRENCE
LIVERMORE
NATIONAL
LABORATORY

Proposed 237U Evaluation for the next ENDL Release

D. Brown, N. Summers, I. Thompson, W. Younes

December 17, 2007

Disclaimer

This document was prepared as an account of work sponsored by an agency of the United States government. Neither the United States government nor Lawrence Livermore National Security, LLC, nor any of their employees makes any warranty, expressed or implied, or assumes any legal liability or responsibility for the accuracy, completeness, or usefulness of any information, apparatus, product, or process disclosed, or represents that its use would not infringe privately owned rights. Reference herein to any specific commercial product, process, or service by trade name, trademark, manufacturer, or otherwise does not necessarily constitute or imply its endorsement, recommendation, or favoring by the United States government or Lawrence Livermore National Security, LLC. The views and opinions of authors expressed herein do not necessarily state or reflect those of the United States government or Lawrence Livermore National Security, LLC, and shall not be used for advertising or product endorsement purposes.

Proposed ^{237}U Evaluation for the next ENDL Release

David Brown, Neil Summers, Ian Thompson, Walid Younes [*]

November 12, 2007

Abstract

We detail the new LLNL evaluation of ^{237}U for inclusion in both the next release of the ENDL and ENDF/B-VII databases. This evaluation is based on a combination of TALYS calculations, data fits and the earlier JEFF-3.1 evaluation. Our evaluation is in excellent agreement with published surrogate (n, f) data [11, 12, 13, 14, 18] and the unpublished LLNL surrogate (n,2n) data [16].

Contents

[*]Lawrence Livermore National Laboratory, Livermore, CA 94550 USA

1 Introduction

^{237}U is an unstable uranium isotope with an 6.75 day half-life. Its short half life makes direct measurement of its properties extremely difficult. To date, only one published direct measurement of its fission cross-section exists [23]. Other integral experiments [20, 22, 19, 25] are equally difficult due to the care that must be taken to characterise the rapidly decaying target material. The dearth of experimental data poses a challenge to creating a faithful evaluation of ^{237}U's neutron induced reactions.

Recently, a re-evaluation of Cramer and Britt's ^{236}U(t, pf) [15] data by Younes et $al.$(Refs. [11, 12, 13, 14]) led to an improved estimate of the ^{237}U(n, f) cross-section. This estimate is in excellent agreement with another surrogate measurement performed by Burke et $al.$ [18] and in reasonable agreement with the direct measurement of McNally et $al.$ [23]. This coupled with the new, unpublished, data from L. Bernstein [16] and the new evaluations in the ENDF/B-VII.0 [4], JEFF-3.1 [5] and JENDL-3.3 [6] data libraries make this an opportune time to re-evaluate ^{237}U.

We now outline this report. First, we review existing evaluations, concentrating on parts of the evaluations we intend to adopt for our new evaluation. Second, we review the available resonance evaluations in some detail and discuss why we adopt the JEFF-3.1 evaluaton. Third, we review direct and integral measures of the ^{237}U(n, f) cross-section. Next, we review the surrogate measurements, concentrating on the Younes et $al.$ [11, 12, 13, 14] work and the Burke et $al.$ [18] sets. Finally, we assemble our hybrid evaluation encapsulating best features of existing evaluations, overall good agreement with existing data, and solid theoretical calculations based on the TALYS reaction code [34].

2 Overview of Evaluations

In this section we present an overview of all of the evaluations for ^{237}U. Table 1 compares the contents of the evaluations and Figures 1 and 2 presents plots of some selected evaluations compared to data.

2.1 Caner, Segev and Yiftah

In 1976, Caner, Segev and Yiftah evaluated the total, elastic, capture, inelastic, and fission cross-sections using Hauser-Feshbach techniques [1]. These results are quite reasonable, but clearly could use tuning to match our current understanding of the fission cross-sections as discussed below.

2.2 ENDL99

No documentation is provided for this evaluation. Furthermore, it is in poor agreement with fission data and total cross-section systematics.

2.3 ENDF/B-VI.8

The ENDF/B-VI.8 is mostly derived from the older ENDL evaluation contained in ENDL99 [7], with a few modifications. The prompt $\bar{\nu}$ data are computed from Gordeeva and Smirenkin [27] and Manero and Konshin [28]. The delayed $\bar{\nu}$ is taken from Brady and England [26]. The resonance parameters are an independent evaluation based on the GENRPAR code of McCrosson [29], the McNally data from LANL [23] and an average level spacing of 3.5 eV.

2.4 ENDF/B-VII.0

The ENDF/B-VII.0 evaluation from LANL [4] was designed to support both reactor and weapons applications. Therefore, it is quite complete. Most of the evaluation results from a single Hauser-Feshbach calculation using the GNASH code system. In fact, the only data files not part of this calculation are the resonance data and the outgoing neutron data from fission, both of which are hold-overs from the ENDF/B-VI evaluation [2]. The evaluators had access to the data of Burke et $al.$ [18] and the evaluation of Younes and Britt [11, 12, 13, 14] so the fission cross-section was tuned to be in excellent agreement with both results.
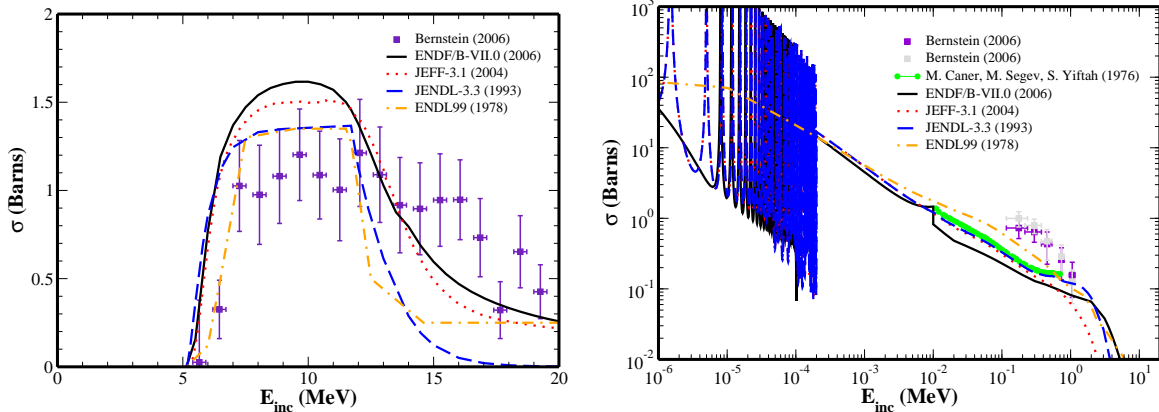
Figure 1: Plots of the (n,2n) and capture cross-section data compared with current evaluations.

The disagreement with the McNally *et al.* [23] is driven by the contamination problem with that data, as noted by Younes and Britt [11, 12, 13, 14], to be discussed below.

2.5 JEFF-3.1

The JEFF-3.1 evaluation in Ref. [5] was constructed at CEA (France) in 2004 in order to support a variety of applications. Thus, it is very complete. The evaluators adopted nearly all of the outgoing particle distributions from the ENDF/B-VIIβ1 evaluation [3] which we assume is the same as the ENDF/B-VII.0 evaluation. The one part not adopted from ENDF/B-VIIβ1 is the outgoing neutrons from fission which the evaluators created from the Vladuca-Tudoro model (a modified Madland-Nix model). The evaluators adopted the high-quality JENDL-3.3 resonance data in total. For the cross-section data, the evaluators performed their own set of Hauser-Feshbach model calculations. This calculation gives a fission cross-section that is in good agreement with the low-energy data of Mc Nally *et al.* [23], but deviates substantially from the later experimental work of Burke *et al.* [18] and Bernstein [16]. It is not clear whether the evaluators were aware of the contamination problem noted by Younes and Britt [11, 12, 13, 14], but the fission cross-section does not track the McNally data in the region with the contamination problem (1-3 MeV).

2.6 JENDL-3.3

The JENDL-3.3 evaluation in Ref. [6] was constructed at JAERI (Japan) in 1993 for reactor simulations. Therefore, the evaluators took great care in developing the resonance and fission data. No effort was made to ensure that the outgoing photon data was complete. Some effort was made to generate the outgoing neutron distributions based on systematics. For the cross-section data, the evaluators performed an independent set of Hauser-Feshbach model calculations. For fission, however, they adopted a fit to the fission data in Ref. [23]. They were unaware of the contamination problem noted by Younes and Britt [11, 12, 13, 14], so this cross-section is not in agreement with the later experimental work of Burke *et al.* [18]. The resonance data in JENDL-3.3 uses a fit to the fission data from Ref. [23].

3 Resonance Data

There are three data sets that were used to determine the resonance region evaluations in JENDL-3.3 and ENDF/B-VI.8: the McNally bomb-shot data [23] and the reactor irradiation measurements of Cornman, Hennelly, and Banick [19], Halperin *et al.* [22] and Cowen *et al.* [20]. The critical assembly measurements of Cowen *et al.* [20] and [25] were of limited usefulness because the neutron flux was higher energy.

3

Reaction	Quantity	(MF, MT)	ENDF/B-VII.0	JEFF-3.1	JENDL-3.3	Data
(n, res)	Thermal	(2, 151)	Adopt [2]	Adopt [6]	FIT	[19, 20, 22]
	RR	(2, 151)	Adopt [2]	Adopt [6]	FIT	[23]
	URR	(2, 151)	Adopt [2]	Adopt [6]	FIT	[23]
(n, tot)	$\sigma(E)$	(3, 1)	HF	HF	HF	None
(n, el)	$\sigma(E)$	(3, 2)	HF	HF	HF	None
	$P_n(E\|\mu)$	(4, 2)	HF	HF	HF	None
$(n, X\gamma)$	$\sigma(E)$	(3, 3)	HF	HF	HF	None
	$M_\gamma(E)$	(13, 3)	HF	HF	HF	None
	$P_\gamma(E\|\mu)$	(14, 3)	HF	HF	HF	None
	$P_\gamma(E\|E')$	(15, 3)	HF	HF	HF	None
(n, γ)	$\sigma(E)$	(3, 102)	HF	HF	HF	[16]
	$M_\gamma(E)$	(12, 102)	HF	Adopt [4]	None	None
	$P_\gamma(E\|\mu)$	(14, 102)	HF	Adopt [4]	None	None
	$P_\gamma(E\|E')$	(15, 102)	HF	Adopt [4]	None	None
(n, n')	$\sigma(E)$	(3, 4, 51-79, 91)	HF	HF	HF	None
	$P_n(E\|\mu)$	(4, 4, 51-79)	HF	HF	HF	None
	$P_n(E\|\mu)$	(4, 91)	None	None	HF	None
	$P_n(E\|E')$	(5, 91)	None	None	SYS	None
	$P_n(E\|\mu, E')$	(6, 91)	None	None	None	None
	$P_\gamma(E\|\mu, E')$	(6, 91)	None	None	None	None
$(n, 2n)$	$\sigma(E)$	(3, 16)	HF	HF	HF	[16]
	$P_n(E\|\mu)$	(4, 16)	None	None	ISO	None
	$P_n(E\|E')$	(5, 16)	None	None	SYS	None
	$P_n(E\|\mu, E')$	(6, 16)	HF	Adopt [4]	None	None
$(n, 3n)$	$\sigma(E)$	(3, 17)	HF	HF	HF	None
	$P_n(E\|\mu)$	(4, 17)	None	None	ISO	None
	$P_n(E\|E')$	(5, 17)	None	None	SYS	None
	$P_n(E\|\mu, E')$	(6, 17)	HF	Adopt [4]	None	None
$(n, 4n)$	$\sigma(E)$	(3, 37)	HF	HF	None	None
	$P_n(E\|E')$	(5, 37)	None	None	None	None
	$P_n(E\|\mu)$	(4, 37)	None	None	None	None
	$P_n(E\|\mu, E')$	(6, 37)	HF	Adopt [4]	None	None
(n, f)	$\sigma(E)$	(3, 18)	HF	HF	FIT+SYS	[18], [23]
	$\nu_{tot}(E)$	(1, 452)	Adopt [2]	SYS	SYS	None
	$\nu_d(E)$	(1, 455)	Adopt [2]	SYS	SYS	None
	$\nu_p(E)$	(1, 456)	Adopt [2]	SYS	SYS	None
	$P_n(E\|\mu)$	(4, 18)	ISO	ISO	ISO	None
	$P_n(E\|E')$	(5, 18)	Adopt [2]	SYS	SYS	None
	$M_\gamma(E)$	(12, 18)	HF	Adopt [4]	None	None
	$P_\gamma(E\|\mu)$	(14, 18)	HF	Adopt [4]	None	None
	$P_\gamma(E\|E')$	(15, 18)	HF	Adopt [4]	None	None

Table 1: Contents of the various evaluations. Here, FIT means fit to available data, SYS means systematics were used, ISO means that the particular angular distribution was assumed to be isotropic, HF means a Hauser-Feshbach and/or Optical Model code was used and None means that data type is not present. If a reference is provided then this refers to the data itself or to another evaluation from which this file was taken.
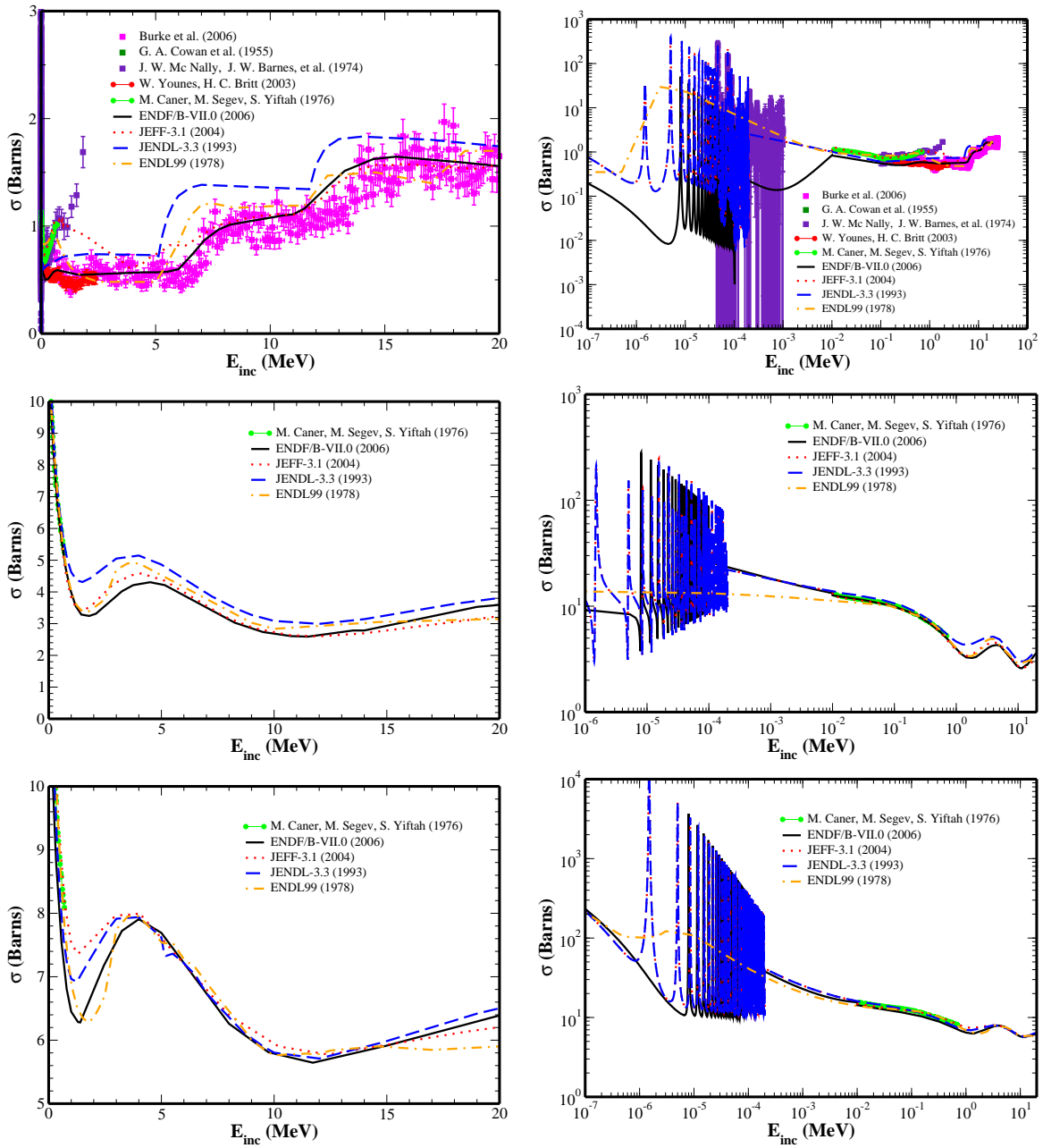
Figure 2: Plots of selected cross-section data compared to current evaluations, on a linear scale (left) and a logrithmic scale (right).

	ENDF/B-VI.8		JENDL-3.3		Data
	σ(0.0253 ev) (barns)	R.I. (barns)	σ(0.0253 ev) (barns)	R.I. (barns)	σ(0.0253 ev) (barns)
Total	487.106	-	478.50	-	-
Elastic	9.131	-	24.39	-	-
Fission	2.000	9.209	1.70	48.7	< 2 [20]
Capture	475.975	309.585	452.40	1080.0	$\approx$ 100 [22]
Absorption	477.975	-	454.10	-	478 $\pm$ 160[19]

Table 2: Calculated thermal cross-sections and resonance integral (R.I.) from the JENDL-3.3 evaluation compared to data from Refs. [19, 20, 22]. Here the absorption channel is the sum of capture and fission channels. The unpublished fission data from Ref. [20] is inconsistent with the JENDL-3.3 evaluation unlike the absorption and capture data from Refs. [19, 22].

The reactor irradiation measurements of Refs. [19], [22] and [20] amounted to placing a ^{237}U foil in front of reactor. This data cannot be used without the incident neutron spectrum, so previous evaluators assumed a thermal neutron spectrum and used these data to set the overall normalization of the resonances.

The detailed resonances were generated using a combination of systematics and the McNally data. In either case, neither of the problems noted by Younes *et al.* [11, 12, 13, 14] were accounted for in their data analysis. In particular, neither the additional 25% ^{237}Np contamination nor the 0.8 factor. This implies that the overall smooth background to the resonance data may need renormalization and several of the ^{237}U resonances may actually be mis-identified ^{237}Np resonances.

None of the datasets strongly favors one resonance evaluation over another. We chose the JENDL-3.3 evaluation only because it matched onto the high energy fission data better.

4 Direct and Integral Fission Measurements

4.1 LANL Integral Measurements

In addition to the reactor irradiation experiment mentioned previously, Cowen *et al.* [20] performed two other irradiation experiments using the neutron flux from the Topsy/Flattop critical assembly (HEU-MET-FAST-028 in Ref. [21]). D. Barr repeated the experiments ([25]) using the second foil prepared for McNally *et al.*, but found different results [23]. The discrepancy between these results is most likely due to the different target composition of the two experiments and is disentangled in [11].

4.2 Direct Measurement Using the Pommard Event

In March 1968, scientists at LANL undertook the most remarkable experiment: they used the Pommard nuclear event as a source of neutrons for irradiating, and measuring the fission cross-section of, ^{237}U. This was a heroic measurement owing both to the activity of the ^{237}U target and the unique nature of the experimental setup, shown in Figure 3.

To produce the ^{237}U target, the McNally *et al.* [23] irradiated a ^{236}U sample in reactor at High Flux Isotopes Reactor (HFIR) at ORNL. The sample was rapidly shipped to LANL where two foils were created. One foil was eventually shipped to the Nevada Test Site for use in the Pommard event and the other remained at LANL for testing. Due to the high activity of the foils, target purity hard to ascertain. The experimenters measured the amount of ^{237}U in the foils by estimating the amount of ^{237}Np (the decay product of ^{237}U). The amount of ^{237}Np was deduced from the number of decay gammas found using a Ge(Li) detector on decay gamma. As a cross-check, the experimenters also performed a radiochemical analysis of the foil used in the Pommard event after the event.

The foil that remained at LANL was used to estimate the fission cross-section by irradiating it with the Flattop critical assembly [25]. The results of this experiment are in disagreement with the previous Cowen
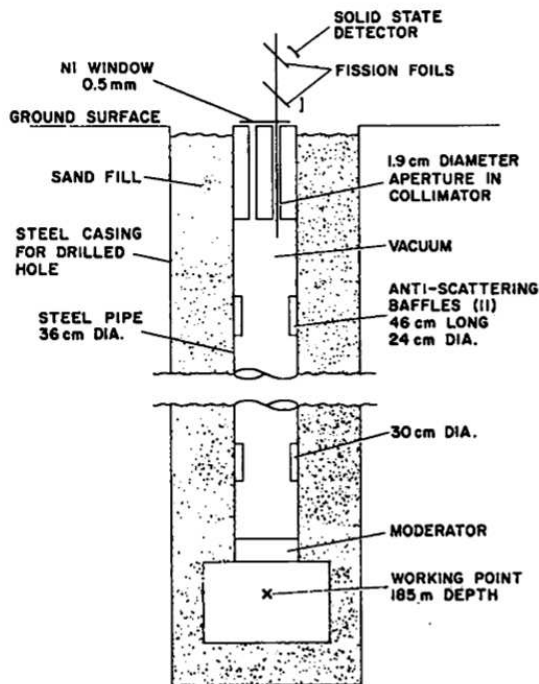
Figure 3: Schematic of Pommard event experimental setup. Reproduction of Fig. 1 from Ref. [24].

et al. experiment [20].

The foil that was used during the Pommard event was placed 185 m above the "working point," along with several other foils including a ^{235}U flux monitor. The samples were irradiated with both the gamma rays from the electromagnetic pulse of the bomb and the fast and moderated neutrons from the source. The neutron incident energy was measured by time of flight, but data taking was lost during $50 - 250$ μsec after the event began, leading to a loss of intermediate energy data. Furthermore, this loss caused an amplifier to drift creating a non-trivial background to the data. In addition, determining the actual flight time of a neutron is complicated by the evolving shape of the source region and the presence of the moderator in the bore-hole. In addition, the electromagnetic pulse ionized the residual gas in the vacuum pipe, creating an additional background. To determine the cross-section, the experimenters counted the number of fissions with a fission counter.

There are numerous potential sources of underestimated uncertainty and error, and this experiment will never be repeated. Given this, Younes *et al.* set out to understand it in order to compare to their own surrogate data. Lynn and Hayes were first to point out a possible scale factor problem [10], but did not provide any reason for it. Younes *et al.* also noted that the rise in the ^{237}U fission cross-section corresponds to the threshold for ^{237}Np(n, f), leading them to suggest that McNally *et al.* underestimated the degree of ^{237}Np contamination in their targets. Using an overall normalization factor of 0.8 and a fractional ^{237}Np contamination of 25%, Younes was not only able to match their estimate of ^{237}U(n, f) onto the McNally measurement, but they were able to match the critical assembly measurements. We will not attempt to justify Younes *et al.* corrections to the McNally data, but we will adopt them and adjust the McNally data accordingly.

7

5 Surrogate Measurements of (n, γ), $(n, 2n)$ and (n, f)

There are two sets of measurements of ^{237}U(n, f) using the Surrogate Method: Cramer and Britt [15] and Burke *et al.* [18]. The earlier measurement by Cramer and Britt was a measurement of ^{236}U(t, pf) which was reanalyzed by Younes *et al.* and reported in a series of papers [11, 12, 13, 14]. The later measurement by Burke *et al.* was a measurement of the ratio ^{238}U$(\alpha, \alpha' f)/^{236}U(\alpha, \alpha' f)$ and then analyzed to produce the ratio ^{237}U$(n, f)/^{235}$U(n, f). Despite the very different spin matchings and reaction mechanisms, both surrogate measurements produce results in excellent agreement with each other and with the corrected McNally data [23]. This agreement between these three completely different approaches gives us confidence in all three. Given this, we fit the combination of all three measurements and used the fit in our evaluation.

Recently, L. Bernstein *et al.* [16] measured the (n, γ) and $(n, 2n)$ cross-sections for ^{237}U using the Surrogate Method on ^{238}U(α, α'). While this data remains preliminary, it is intriguing since the capture cross-section is comparable to or slightly larger than the fission cross-section around 200 keV. However, we caution that since this data is preliminary, we compare to it, but do not tune our evaluation to match them. The $(n, 2n)$ data compares favorably with the fission-competition-corrected TALYS calculations, however the (n, γ) appears to be about a factor of 2-4 too high. It is possible to tune our capture results to match the Bernstein data, but we are hesitant to do so before the data progresses out of its current preliminary state.

There are several possible reasons for the disagreement, and we list them here:

- The absolute normalization may be off due to the overly complicated data analysis of emitted gammas. We doubt this could account for a factor of 2.

- The energy gets shifted in the reworking of $(\alpha, \alpha' X)$ to (n, X). A fix here might improve the agreement with the $(n, 2n)$ near threshold and reduce the disagreement between the (n, g) data from a factor of 4 to a factor of 2.

- The spin distribution in the surrogate reaction may be a poor match to the compound formation reactionsurrogate formation.

- The capture measurements have an equivalent measurement that corresponds to neutron energies in which the width fluctuation correction (WFC) is important. Previous experience shows us that the WFC tends to lower the capture cross-section and raise the other reaction channel cross-sections. Indeed, since the measured data was actually a ratio to fission, the ratio should be lowered twice over because of the WFC. Since it is difficult to predict the magnitude of the WFC and because of its energy dependence, we will ignore the surrogate (n, γ) data. However test calculations show that this does not explain the result.

6 Assembly of the Hybrid Evaluation

We now describe how we generated our ^{237}U evaluation. First we detail our fit to the ^{237}U(n, f) cross-section. Second, we describe the TALYS calculations that we performed to generate the high-energy cross-section data and outgoing neutron data. Third, we detail the adjustments we made to the cross-section data in order to properly account for the change in the competition with the fission channel caused by the use of our fit to the fission data as well as the modification to the reaction cross-section that we did. This will allow us to compare our predictions of the $(n, 2n)$ and (n, γ) cross-sections with the data of Bernstein [16]. Finally, we list the components from other evaluations that we adopt as part of this evaluation.

6.1 Determining the (n, f) Cross-section

To determine the ^{237}U(n, f) cross-section, we performed a generalized least-square fit of a linear spline to the combined data sets of Burke, *et al.* [18], (corrected) McNally *et al.* [23], and Cramer and Britt [15] as interpreted by Younes *et al.* [11, 12, 13, 14]. Figure 4 shows our fit. The linear spline is defined on the interval 0.1 - 20 MeV with 24 knots and 22 fit coefficients. The final χ^2 is 526 giving a χ^2 per degree of freedom of 2.38. It is possible to improve the quality of the fit, but we felt the issues with the various experiments did not merit the improved fit quality.
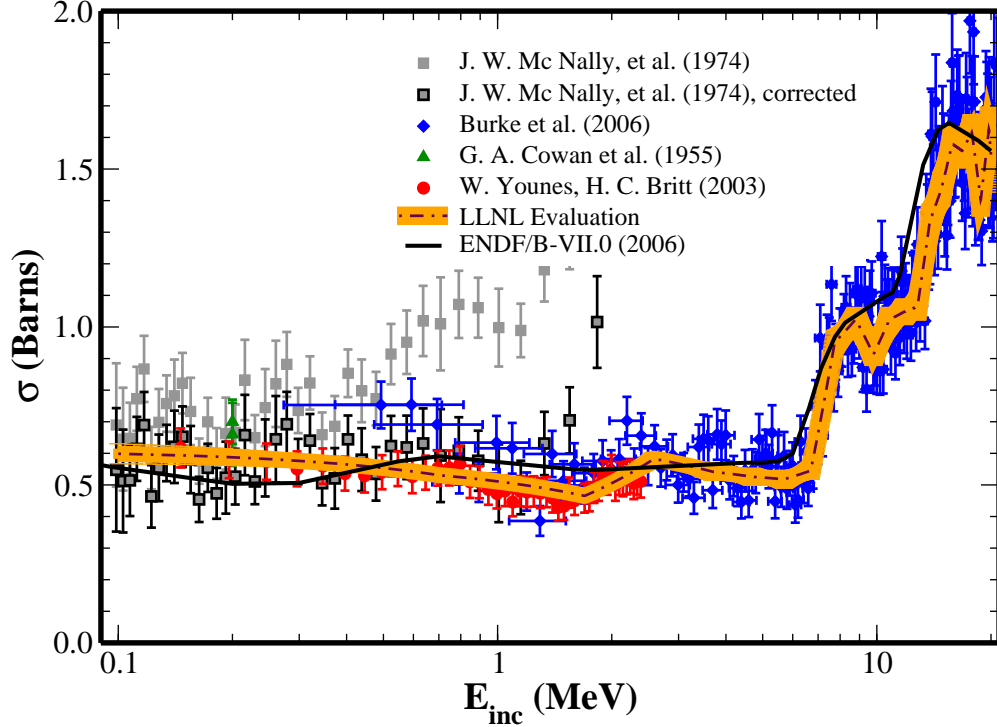
Figure 4: Generalized least-squares fit to surrogate and absolute ^{237}U(n, f) data.

6.2 Calculating the Other Cross-Sections and Outgoing Particle Distributions Using TALYS

To calculate the remaining cross sections, as well as the outgoing particle distributions, the Hauser-Feshbach code TALYS [34] was used. The RIPL-2 database included in the TALYS distribution provided the masses, level scheme, and discrete γ-ray data.

The neutron channels were calculated by using the optical potential of Soukhovitski, Chiba, *et al.* [35], which was fitted to use deformation lengths of $\delta_2 = 1.75$ fm and $\delta_4 = 0.65$ fm to couple the ground state to the excited states 1, 2, 3 and 5 (spins $1/2^+$ through $9/2^+$). (The default TALYS calculation also calculates DWBA octupole transitions to three negative parity states around 0.55 MeV, but these were removed [39].)

The proton transmission coefficients use the optical potentials of Koning and Delaroche [36], and the deuteron potential is constructed as the sum of neutron and proton potentials at half the deuteron incident energy. The density of the compound nuclear states was calculated by the method of Gilbert and Cameron [37], from the Fermi Gas model above 2.6 MeV and the constant temperature model below that energy. The density parameters were $a = 20.297$ for ^{237}U, and $a = 20.675$ for ^{238}U, with $\Delta = 0.779$ and 1.555 respectively. The γ-ray strength function used the Kopecky-Uhl model [38] for E1 transitions, renormalised by a factor of 1.202 to reproduce the experimental total radiative width of 0.03 eV. Pre-equilibrium reactions were simulated using a two-component exciton model with cluster emission, using nn matrix elements enhanced by a factor of 1.5 over the other isotopic combinations.

We further note that the `fudge fixQandThreshold()` function was used to bring thresholds and Q values in synchronization with masses from the Audi Wapstra 2003 atomic mass evaluations. We also encountered a bug in TALYS that allows outgoing particles with energy $E' < E + Q - X1$, exceeding what is physically possible. This seems to be an artifact of the way TALYS bins the outgoing particle distributions. Finally, we discarded any reactions whose maximum was < 1 % of maximum compound elastic cross-section
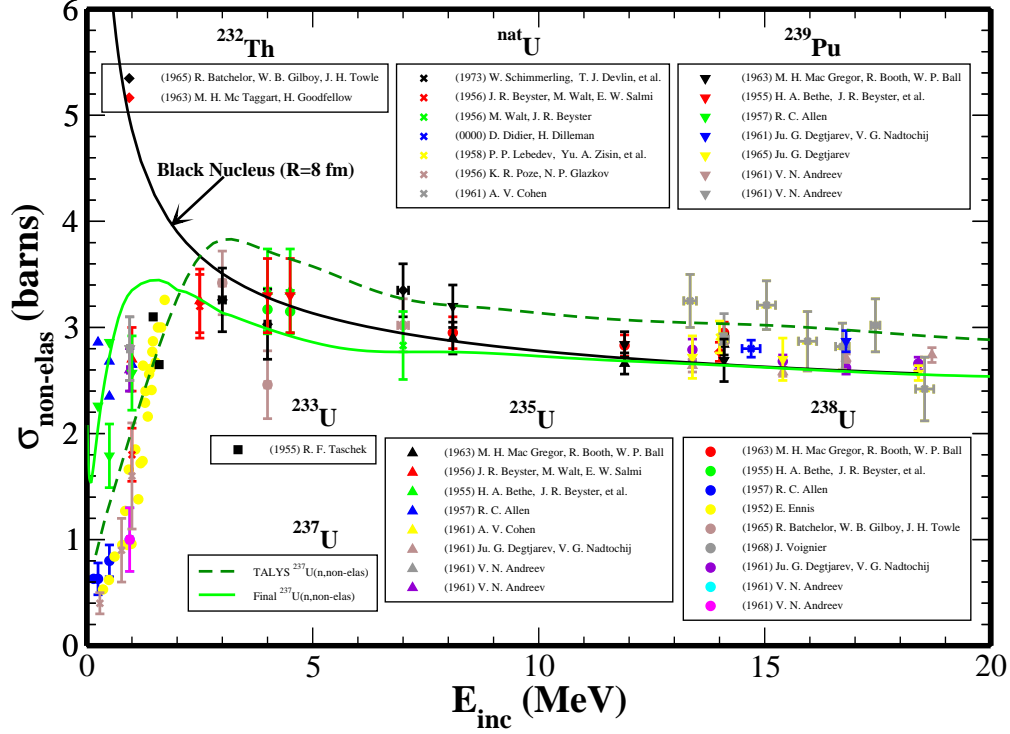
Figure 5: Plot showing the world's collection of actinide non-elastic cross-section measurements, along with the TALYS calculations used in thie evaluation. The Black Nucleus curve is also included for reference.

6.3   Accounting for Fitted Fission Cross-Section and TALYS's Poor Agreement with Non-Elastic Cross-Section Data

The TALYS calculations just described, when combined with the default fission barriers, have two short-comings. First, they do not match the fits to the fission cross-section performed above. They also do not match the systematics for the non-elastic cross-sections on actinides as shown in Figure 5. These non-elastic cross-section measurements are difficult neutron transmission experiments and thus potentially untrustworthy. However, they do indicate that the TALYS non-elastic cross-section is systematically high. Indeed, since this cross-section is the reaction cross-section minus the compound elastic cross-section, this cross-section is controlled by the gross behavior of the imaginary part of the optical model potential (or the equivalent coupled channel calculation). Thus, it is dominated by the gross shape of the nucleus except at the lowest energies (< 2 MeV) where structure effects become important. Given the nuclear structure similarities between ^{235}U and ^{237}U, we would expect that the non-elastic cross-section for ^{237}U should track the ^{235}U data below 2 MeV.

Given these two shortcomings, we now describe how we remedy them. First, we note that the various reaction cross-sections all sum to form the total reaction cross-section:

$$\sigma_{rxn} = \sigma_{\text{comp-elas}} + \sigma_{\text{fis}} + \sigma_{(n,2n)} + ... = \sum_x \sigma_x, \tag{1}$$

where the non-elastic cross-section is $\sigma_{\text{non-elas}} = \sigma_{rxn} - \sigma_{\text{comp-elas}}$. We wish to replace the incorrect reaction and fission cross-sections σ_{rxn} and σ_{fis} with corrected ones σ'_{rxn} and σ'_{fis}, while maintaining the correct inter-channel competition from TALYS.

If we define "partial widths" as $\Gamma'_x = \sigma_x/(\sigma_{rxn} - \sigma_{\text{fis}})$, these Γ'_x should be preserved as they describe the inter-channel competition in TALYS. To be compatible with the correct σ'_{rxn} and σ'_{fis} cross sections, the

10
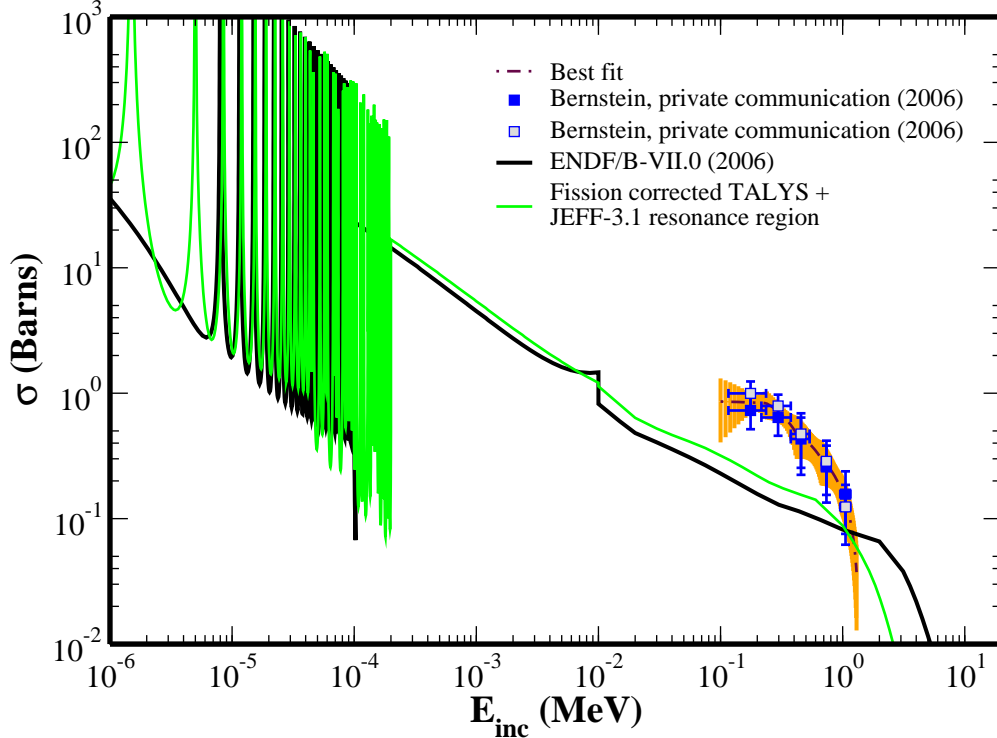
Figure 6: Our evaluation of the (n, γ) reaction.

other channels x should therefore be simultaneously corrected according to

$$\sigma'_x = \sigma_x \left(\frac{\sigma'_{rxn} - \sigma'_{\text{fis}}}{\sigma_{rxn} - \sigma_{\text{fis}}} \right). \tag{2}$$

This result can be made rigorous in the Weisskopf-Ewing limit.

The result of this adjustment can be seen in Figures 6 and 7. We arrive at an $(n, 2n)$ cross-section that is in reasonable agreement with the surrogate measurement of Bernstein *et al.*, but is significantly lower than their (n, γ) cross-section. This difference is now under study by Bernstein *et al.* and, if the capture data proves to be correct, we will adjust either the appropriate gamma ray strength function in TALYS or the reaction cross section to achieve a better match.

6.4   Files Adopted from Other Evaluations

TALYS, being a nuclear reaction code, has no capability to produce resonance data. It also does not have a model for the outgoing fission neutron spectrum or $\bar{\nu}$. Finally, because we used software tools that are still in active development, we were also unable to translate the TALYS gamma data into either ENDL or ENDF format. All these elements are present in the JEFF-3.1, JENDL-3.3 and ENDF/B-VII.0 evaluations as they are required of all ENDF evaluations. So, we adopted all of these from the JEFF-3.1 evaluation. Table 3 summarizes our choices.

Acknowledgments

11
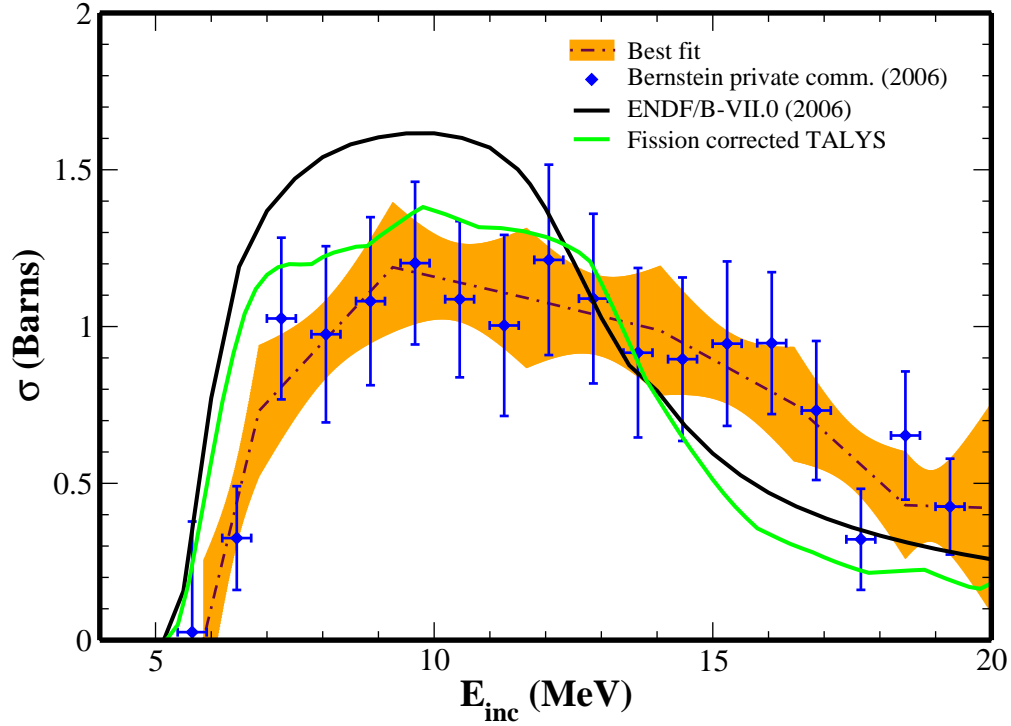
Figure 7: Our evaluation of the $(n, 2n)$ reaction.

MF	MT	Data type	Reason
2	151	Resonance region	See section 3
1	452	Total fission $\bar{\nu}$ data	New JEFF-3.1 evaluation
1	455	Delayed fission $\bar{\nu}$ data	New JEFF-3.1 evaluation
5	455	Delayed fission neutron spectrum	New JEFF-3.1 evaluation
1	456	Prompt fission $\bar{\nu}$ data	New JEFF-3.1 evaluation
4	18	Fission neutron angular distribution	New JEFF-3.1 evaluation
5	18	Fission neutron spectrum	New JEFF-3.1 evaluation
12	18	Fission γ multiplicity	New JEFF-3.1 evaluation
14	18	Fission γ angular distribution	New JEFF-3.1 evaluation
15	18	Fission γ spectrum	New JEFF-3.1 evaluation
12	102	Capture γ multiplicity and discrete spectrum	Cannot parse TALYS γ data yet
14	102	Capture γ angular distribution	Cannot parse TALYS γ data yet
15	102	Capture γ continuous spectrum	Cannot parse TALYS γ data yet
13	3	C = 55 γ production cross-sections	Cannot parse TALYS γ data yet
14	3	C = 55 γ angular distribution	Cannot parse TALYS γ data yet
15	3	C = 55 γ continuous spectrum	Cannot parse TALYS γ data yet

Table 3: Files adopted from the JEFF-3.1 evaluation for use in our ^{237}U evaluation.

A   Evaluation Documentation

D.A. Brown, N. Summers, I. Thompson, W. Younes

MF=1 General Information

   Taken from JEFF-3.1.

   MT=452 Total Nubar. Sum of MT=455 and 456
   MT=455 Delayed Neutron Yields, taken from Ref. [2]
          and is given in 8 delayed neutron groups.
   MT=456 Prompt Neutron Yields.
          Vladuca and Tudora BRC improved Madland-Nix model
   MT=458 Not given

   The prompt fission neutron multiplicity and spectra
   are calculated using the BRC improved Los Alamos model from
   Vladuca and Tudora [1]. The model parameters are slightly
   different from those adopted in [1]. The prompt fission
   neutron multiplicity is obtained from an energetic balance
   ratio. The available energy (the average fission energy
   released minus the average fission fragment kinetic energy
   minus the average prompt gamma ray energy) is divided by the
   energy carry away by the neutron (the average fission
   fragment neutron separation energy plus the average
   center-of-mass energy of the emitted neutrons). The main
   improvement is the dependence of the average total
   fission-fragment kinetic energy and the average gamma energy
   on neutron incident energy.

MF=2, MT=151 Resonance Parameters

   Taken from JEFF-3.1 (which adopts JENDL-3.3 parameters).

   1) Resolved Resonance Parameters: MLBW (1.0e-5 - 200 ev)
      below 45 ev, hypothetical resonances were generated from
      fission width of 0.004 ev, s0 of 1.0e-4 and level spacing o
      3.5 ev, and adjusted to reproduce thermal cross sections.
      above 46 ev, parameters were estimated from fission-area
      data measured by McNally et al. [3]

   2) Unresolved Resonance Parameters: 200 ev - 30 kev
      obtained by fitting to capture and fission cross sections
      with ASREP [4].
          S0 and S2 = (0.97 - 1.02)e-4, S1 = (1.95 - 2.04)e-4,
          Gamma-f = (0.006 - 0.070) ev, Gamma-g = 0.035 ev
          R = 9.668 fm

```
   Calculated thermal cross sections and res. integral (barns)
             0.0253 ev       resonance integral
                (barns)            (barns)
     Total         478.50              -
     Elastic        24.39              -
     Fission         1.70             48.7
     Capture       452.40           1080.0
```

Unresolved Resonance Range 10 keV to 30 keV :
The four energy dependant widths parameters originally
described in JENDL-3.3 have been removed to account for
direct interaction on the first inelastuc level

MF=3 Cross-section data

  New LLNL evaluation

  MT=18:   Generalized least squares fit to data
  Other MT's: Taken from calculations using TALYS-0.72,
              including correction for inter-channel
              competition.

  To determine the 237U(n,f) cross-section, we performed a
  generalized least-square fit of a linear spline to the
  combined data sets of Burke,   et al. [5], (corrected)
  McNally et al. [3], and Cramer and Britt [6] as interpreted
  by Younes et al. [7]. The linear spline is defined on the
  interval 0.1 - 20 MeV with 24 knots and 22 fit coefficients.
  The final chi^2 is 526 giving a chi^2 per degree of freedom
  of 2.38. It is possible to improve the quality of the fit,
  but we felt the issues with the various experiments did not
  merit the improved fit quality.

  To calculate the remaining cross sections, as well as the
  outgoing particle distributions, the Hauser-Feshbach code
  TALYS [8] was used. The RIPL-2 database included in the
  TALYS distribution provided the masses, level scheme, and
  discrete gamma-ray data.

  The neutron channels were calculated by using the optical
  potential of Soukhovitski, Chiba, et al. [9], which was
  fitted to use deformation lengths of delta_2 = 1.75 fm and
  delta_4 = 0.65 fm to couple the ground state to the excited
  states 1, 2, 3 and 5 (spins 1/2+ through 9/2+). (The default
  TALYS calculation also calculates DWBA octupole transitions
  to three negative parity states around 0.55 MeV, but these
  were removed.)

  The proton transmission coefficients use the optical
  potentials of Koning and Delaroche [10], and the deuteron
  potential is constructed as the sum of neutron and proton
  potentials at half the deuteron incident energy. The density

                          14

of the compound nuclear states was calculated by the method
of Gilbert and Cameron [11], from the Fermi Gas model above
2.6 MeV and the constant temperature model below that energy.
The density parameters were a=20.297 for 237U, and a=20.675
for 238U, with Delta= 0.779 and 1.555 respectively. The
gamma-ray strength function used the Kopecky-Uhl model [12]
for E1 transitions, renormalised by a factor of 1.202 to
reproduce the experimental total radiative width of 0.03
eV. Pre-equilibrium reactions were simulated using a
two-component exciton model with cluster emission, using
nn matrix elements enhanced by a factor of 1.5 over the
other isotopic combinations.

The TALYS calculations as described did not reproduce either
the measured fission data or non-elastic cross-section
systematics for the actinides. So, we replace the TALYS
fission cross-section, sigma_fis, with our fit, sigma_fis',
and we adjusted the TALYS reaction cross-section sigma_rxn.
Our new reaction cross-section, sigma_rxn', lowers the TALYS
non-elastic cross-section above 3 MeV to be consistent with
actinide systematics and raises it below 2 MeV to be
consistent with 235U non-elastic measurements in this
energy range. To be compatible with the correct sigma_rxn'
and sigma_fis' cross sections, the other channels x are
simultaneously corrected according to
      sigma_x' = sigma_x * [(sigma_rxn'-sigma_fis') /
                                (sigma_rxn-sigma_fis)].
This result can be made rigorous in the Weisskopf-Ewing limit.

MF=12 Photon Production Multiplicities

   Taken from JEFF-3.1 (which adopts ENDF/B-VII.0 data).

   MT=18   Taken from GNASH calculations in ENDF/B-VII.0
   MT=102 Taken from GNASH calculations in ENDF/B-VII.0

MF=13 Photon Production Cross-section

   Taken from JEFF-3.1 (which adopts ENDF/B-VII.0 data).

   MT=3   Taken from GNASH calculations in ENDF/B-VII.0

MF=14 Photon Angular Distribution

   Taken from JEFF-3.1 (which adopts ENDF/B-VII.0 data).

   MT=3   Taken from GNASH calculations in ENDF/B-VII.0
   MT=18   Taken from GNASH calculations in ENDF/B-VII.0
   MT=102 Taken from GNASH calculations in ENDF/B-VII.0

```
MF=15   Continuous Photon Energy Spectra

   Taken from JEFF-3.1 (which adopts ENDF/B-VII.0 data).

   MT=3     Taken from GNASH calculations in ENDF/B-VII.0
   MT=18    Taken from GNASH calculations in ENDF/B-VII.0
   MT=102   Taken from GNASH calculations in ENDF/B-VII.0


   ------------------------------------------------------------------
   References

[1] G. Vladuca and A. Tudora, Ann. Nuc. Energy. 28, 689 (2001).

[2] Y. Rugama (NEA/OECD), Jefdoc-976 (2001); Wilson and England,
    Prog. Nucl. Eng. 41, 71 (2002).

[3] J.H.Mcnally et al., Phys. Rev., C 9, 717 (1974).

[4] Y.Kikuchi: unpublished.

[5] J.T. Burke, L.A. Bernstein, J. Escher, et al. Phys. Rev.
    C 73, 054604 (2006).

[6] J.D. Cramer, H.C. Britt, Nucl. Sci. Eng. 41, 177 (1970).

[7] W. Younes, H.C. Britt, "Estimates of the 237,239U(n,f)
    cross sections for 0.1 < En(MeV) <= 20," LLNL Report
    UCRL-TR-212600 (2005).

[8] A. Koning, S. Hilaire, M. Duijvestijn, TALYS Reaction Code
    version 0.72 (2007).

[9] Soukhovitski, Chiba, et al., J. Phys. G: Nucl. Part. Phys.
    30, 905 (2004).

[10] A.J. Koning and J.P. Delaroche, Nucl. Phys. A713, 231 (2003).

[11] A. Gilbert and A.G.W. Cameron, Can. J. Phys. 43, 1446 (1965).

[12] J. Kopecky and M. Uhl, Phys. Rev. C 42, 1941 (1990).
```

References

[1] M.Caner, M.Segev, S.Yiftah, Nucl. Sci. Eng. **59**, 395 (1976); EXFOR Entries V0005002, V0005003, V0005004, V0005005, V0005006.

[2] Kinsey, ENDF/B-VI release 8 Material 9234 (1976).

[3] P.G. Young, M.B. Chadwick, LANL internal report T-16:NW-2/10-00; ENDF/B-VIIβ1 Material 9234 (2004).

[4] P.G. Young, M.B. Chadwick, ENDF/B-VII.0 Material 9234 (2006).

[5] Lopez, Jimenez, Morillon, Romain, JEFF-3.1 Material 9234 (2004).

[6] T. Nakagawa, JENDL-3.3 Material 9234 (1993).

[7] R. Howerton, LLNL Report UCRL-50400 Vol. 15, Part A, Sept 1975 (Methods) and Part B, Apr 1976 (Curves).

[8] D. A. Brown, D. P. McNabb, B. Beck, LLNL Report UCRL-TR-202393 (2004).

[9] V. M. Maslov, "^{237}U neutron-induced fission cross section," Phys. Rev. C **72**, 044607 (2005).

[10] J. E. Lynn, A. C. Hayes, "Theoretical evaluations of the fission cross section of the 77 eV isomer of ^{235}U," Phys. Rev. C **67**, 014607 (2003).

[11] W. Younes, H.C. Britt, J.B. Wilhelmy, "The ^{237}U(n, f) Cross Section," LLNL Report UCRL-ID-152621 (2003).

[12] W. Younes, H.C. Britt, J.A. Becker, J.B. Wilhelmy, "Initial estimate of the ^{237}U(n, f) cross section for $0.1 < E_n$(MeV)≤ 20," LLNL Report UCRL-ID-154194 (2003); W. Younes, H.C. Britt, "Estimates of the 237,239U(n,f) cross sections for 0.1 ¡ En(MeV) ¡= 20," UCRL-TR-212600 (2005).

[13] W. Younes, H.C. Britt, "Neutron Fission of ^{235,237,239}U and ^{241,243}Pu: Cross Sections, Integral Cross Sections and Cross Sections on Excited States," LLNL Report UCRL-ID-154206 (2003).

[14] W. Younes, H. C. Britt, "Simulated neutron-induced fission cross sections for various Pu, U, Th isotopes," Phys. Rev. C **68**, 034610 (2003).

[15] J.D. Cramer, H.C. Britt, Nucl. Sci. Eng. **41**, 177 (1970).

[16] L. Bernstein, *et al.*. "Deducing the ^{237}U(n, γ) and $(n, 2n)$ cross-sections using a new Surrogate Ratio Method," in preparation (2007).

[17] C. Plettner, H. Ai, C.W. Beausang, L.A. Bernstein, L. Ahle, H. Amro, M. Babilon, J.T. Burke, J.A. Caggiano, R.F. Casten, J.A. Church, J.R. Cooper, B. Crider, G. Gürdal, A. Heinz, A. McCutchan, K. Moody, J.A. Punyon, J. Qian, J.J. Ressler, A. Schiller, E. Williams, W. Younes, Phys. Rev. C **71**, 051602(R) (2005).

[18] J.T. Burke, L.A. Bernstein, J. Escher, *et al.*, "Deducing the ^{237}U(n, f) cross section using the surrogate ratio method," Phys. Rev. C **73**, 054604 (2006); EXFOR Entry 14094002.

[19] W.R. Cornman, E.J. Hennelly, C.J. Banick, Nucl. Sci. Eng. **31**, 149 (1968); EXFOR Entry 12455002.

[20] G.A. Cowen, G.A. Jarvis, G.W. Knobeloch, B. Warren, LANL Report LA-1669 (1955); EXFOR Entry 12500002.

[21] Ed. B. Briggs, "International Handbook of Evaluated Criticality Safety Benchmark Experiments," NEA/NSC/DOC(95)03 (2007).

[22] J. Halperin, J.J. Pinajian, C.R. Baldock, J.H. Oliver, R.W. Stoughton, ORNL Report ORNL-3994, p. 1, (1966); EXFOR Entry 13016002.

[23] J.W. Mc Nally, J.W. Barnes, B.J. Dropesky, *et al.*, Phys. Rev. C 9, 717-722 (1974); EXFOR Entry 10059002; P.A. Seeger, LANL Report LA-4420 (1970).

[24] W.K. Brown, P.A. Seeger, M.G. Silbert, LANL Report LA-4095 (1970).

[25] D. Barr, private communication (as reported in Ref. [23]).

[26] M.C.Brady, T.R.England, Nucl. Sci. Eng. **103**, 129 (1989).

[27] L.D.Gordeeva, G.N.Smirenkin, Sov. At. En. 14, p. 56 (1963).

[28] F. Manero, V.A. Konshin, At. En. Rev. 10, p. 637 (1972).

[29] F.J. McCrosson, Proc. Conf. Neut. Cross Sections and Tech., Knoxville, TN, p.714 (1971).

[30] D.A. Brown, N. Summers, I. Thompson, "Proposed 236U Evaluation for the next ENDL Release," LLNL Report UCRL Pending (2007).

[31] N. Summers, `geft`, private communication (2007).

[32] D.A. Brown, `endl2endf`, private communication (2007).

[33] B. Beck, `fudge`, private communication (2007).

[34] A. Koning, S. Hilaire, M. Duijvestijn, TALYS Reaction Code version 0.72.

[35] E. Sh Soukhovitskii, S. Chiba, J.-Y. Lee, O. Iwamoto and T. Fukahori, J. Phys. G: Nucl. Part. Phys. 30, 905 (2004).

[36] A.J. Koning and J.P. Delaroche, Nucl. Phys. A713, 231 (2003).

[37] A. Gilbert and A.G.W. Cameron, Can. J. Phys. 43, 1446 (1965).

[38] J. Kopecky and M. Uhl, Phys. Rev. C 42, 1941 (1990).

[39] A.J. Koning, private communication (2007).